Title

Evaluating the Ear for Monitoring Somatosensory Evoked Potentials

Authors

Cao, Mingfeng

Uppal, Abhinav

Lee, Min Suk

et al.

Publication Date

2024-06-28

DOI

10.1109/memea60663.2024.10596764

Evaluating the Ear for Monitoring Somatosensory Evoked Potentials

Mingfeng Cao*
Dept. of Biomedical Engineering
Johns Hopkins University
Baltimore, USA
mcao10@jhu.edu

Abhinav Uppal*
Dept. of Bioengineering
UC San Diego
La Jolla, USA
auppal@ucsd.edu

Min Suk Lee
Dept. of Bioengineering
UC San Diego
La Jolla, USA
msl052@ucsd.edu

Prachi Agarwal
Dept. of ECE
Johns Hopkins University
Baltimore, USA
pagarwa7@jhu.edu

Rommani Mondal
Dept. of Bioengineering
UC San Diego
La Jolla, USA
rmondal@ucsd.edu

Sangjoon An
Dept. of Bioengineering
UC San Diego
La Jolla, USA
s5an@ucsd.edu

Akshay Paul
Inst. for Neural Computation
UC San Diego
La Jolla, USA
a1paul@ucsd.edu

Yuchen Xu
Inst. for Neural Computation
UC San Diego
La Jolla, USA
yux013@ucsd.edu

Gert Cauwenberghs
Dept. of Bioengineering
UC San Diego
La Jolla, USA
gert@ucsd.edu

Nitish V. Thakor
Dept. of Biomedical Engineering
Johns Hopkins University
Baltimore, USA
nitish@jhu.edu

***Abstract*—Short-latency somatosensory evoked potentials (SSEPs) serve as a biomarker for recovery of consciousness from coma but often require bulky and time-consuming measurement setups such as scalp-based electroencephalography (EEG), cervical recording, or invasive in-vivo electrodes, which limits their deployment to clinical environments. To extend the utility of SSEPs in ambulatory monitoring and acute care, here we present a pilot study recording SSEPs from the inside of the ears of three rat subjects tested using non-invasive silver / silver-chloride (Ag / AgCl) electrodes. Simultaneous recording from stainless steel electrodes surgically implanted at the cortical surface served as ground truth. The ground electrode for both modalities is shared and placed at 2 mm behind the lambda. The rat subjects under anesthesia using isoflurane were stimulated at the center of the gastrocnemius muscle in the left or right hindlimbs with a pulse width of 200 µs and amplitude of 1 mA every 2 s. Time domain analysis was performed to get epoch-averaged SSEP waveforms from the ear and cortical surface electrodes. Frequency domain analysis reveals that the ear EEG recording is able to capture most characteristics of neural activities below 100 Hz but with a shorter latency of SSEP peaks, warranting further evaluation of ear SSEPs to study if they can reflect experimentally induced changes in the subject state.**

***Index Terms*—EEG, SSEP, rodent, Ear EEG**

I. Introduction

The neural response elicited by the peripheral nerve stimulation is the somatosensory evoked potential (SEP). The SEP has been standardized as a prognostic marker in several clinical conditions and is usually analyzed by characterizing peaks, which are classified according to their polarity and latency after the stimulus in healthy individuals [1]. Short-latency somatosensory evoked potential (SSEP) peaks are those present shortly after stimulation and reflect neural activity at locations closer to the site of stimulation, which are the most consistent when measured in healthy populations. Hence, they are reliable markers in the investigation of the neurological state during clinical practices [2].

There are distinct features of the SSEP that have been identified as pertinent to neuroprognostication [2]. For example, the N20 peak in humans, which is the negative cortical peak occurring 20 ms after stimulation, is one of the several characteristics of the SSEP waveform that have been established as a robust indicator of post-cardiac arrest neurological state. The bilateral absence of the N20 specifically is a hallmark predictor of poor post-cardiac arrest and postanoxic comatose patient outcomes [3], [4]. Time-frequency analysis reveals that SSEP also contains high-frequency components that characterize the recovery of arousal [5].

Traditionally, SSEP recordings are done either non-invasively by placing electrodes on the scalp and/or the cervical skin or invasively in the intracranium, ventricle pathway, cervical spinal cord, etc [6], [7]. However, such recordings can require lengthy setup time, be potentially dangerous to the subject, have an obtrusive interface to the subject, and be unfamiliar and uncomfortable [8]. Therefore, we propose to expand the knowledge of measuring SSEP from a familiar and commonly wearable location around which SSEPs have been observed, the ear [9].

The ear canal is an attractive area for monitoring neurologi-

* These authors contributed equally to this work.

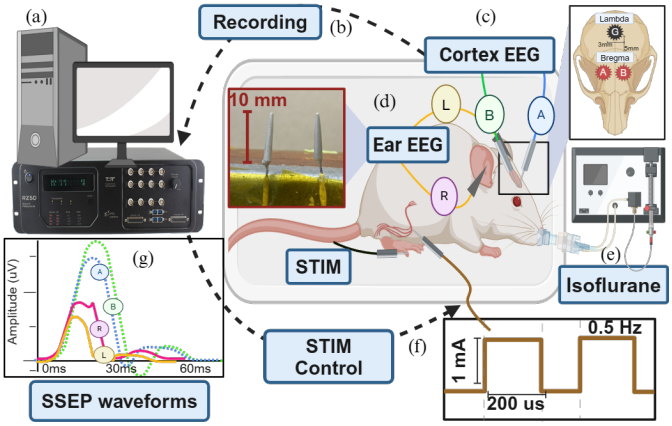

Fig. 1. Schematic picture of the proposed method composed of (a) neural recording and stimulation setup using RX5 TDT device. (b) Placements for EEG recording electrodes in cortex and ear (c) The position of electrodes are marked on an illustration of a rat skull: electrodes A and B were placed on the primary somatosensory cortex hindlimb regions (anterior/posterior (AP): -2; midline/lateral (ML): ± 2). Ground (G) was placed on top of the midline (AP: -5). (d) The hardware of the ear EEG and the electrode placement inside the ear canal, (e) following local anesthetic administration. (f) Placement of SSEP STIM (stimulation) electrodes. (g) Example of SSEP response tracing post-stimulus for cortical (A, B) and ear (L, R) electrodes. Created with Biorender.com.

cal conditions due to its close proximity to the central nervous system and the surrounding vasculature [10]. Information that is crucial for neurocritical care, such as heart rate and oxygen saturation, can be extracted from an ear EEG even in pathological conditions [11]. Ear EEG reflects neural activity from sources that can also be captured by traditional scalp EEG, but in an unobtrusive manner while retaining signal quality [12], [13]. Hence, in ambulatory and sensitive care conditions, the convenience of monitoring EEG from the ear may provide a solution to overcome the circumstantial difficulties of EEG measurement [2], [11]. Ear EEG has several advantages over the traditional modalities in that it is unobtrusive, located close to the subcortical activity, mechanically holds the electrodes in place, and is comfortably familiar for wearables [14], [15].

We believe that an eventual wearable device that is capable of monitoring SSEP unobtrusively will greatly enable data collection and further aid in diagnosis in various environments such as during ambulatory recording, hypothermia, or other procedures when the scalp is not feasible [16]. Conducting a feasibility trial on ear EEG somatosensory evoked response in rats serves as an initial step before translating to human studies. Rats provide a controlled and ethical environment for preliminary investigations, allowing us to refine methodologies and assess the viability of ear SSEP. This approach helps establish the foundation for future translational research in humans, ensuring safety and efficacy and optimizing protocols before implementation in larger clinical studies.

The rest of this paper is organized as follows: Section II describes ear electrode fabrication, SSEP recording protocols in rodents, and signal processing methods used. Section III reports the analysis results, followed by a discussion in Section IV with implications for future investigations.

II. Methods and Measurements

A. Ear Electrode Fabrication

The electrodes used for the ear EEG recording were Ag/AgCl. The Ag/AgCl electrodes were fabricated by first shaping a truncated cone using a 10 Gauge 99.99% Pure Silver Wire and a lathe. The specific dimensions of the truncated cone are shown in Fig. 1. Second, the Ag/AgCl Ink CI-4025 (Nagase ChemteX, Delaware, OH, USA) was coated around the silver substrate. Third, the coated electrodes are then cured by heating at 80°C for 30 minutes in a convection oven to distribute the heat evenly. Lastly, the electrodes are taken out to cool at room temperature for 30 minutes [17].

B. SSEP Recording Protocols

Three adult male Wistar rats aged from 24 to 26 weeks were included in the experiment. Epidural screw electrodes (E363/20, P1 Technologies, Roanoke, VA, USA) were surgically implanted in subjects a week prior to the experiments. Two frontal electrodes were placed 2 mm behind and 2 mm to the side of the bregma (left A; right B), while one ground electrode was placed 2 mm behind the lambda. The TDT data acquisition system (Tucker-Davis Technologies, Alachua, FL, USA) was used to sample SSEPs at a conservatively high rate of 12.207 kHz to preserve potential high-frequency information found in previous studies [5]. SSEPs were stored in the epoch format. Hardware notch filters at 60 Hz, 120 Hz, and 180 Hz were applied.

In order to provide stimulation, a stainless steel electrode (F-E2-48, Natus, Gort, Ireland) was inserted into the center of the gastrocnemius muscle in the left or right hindlimb. Stimulation pulses were 200 µs long, had an amplitude of 1 mA, and were delivered at a frequency of 0.5 Hz.

On the day of the experiment, the rat subject was ventilated with 50%:50% N_2/O_2 containing 3% isoflurane for 2 minutes to induce anesthesia (Piramal Critical Care, West Drayton, UK). Then, 1.8% isoflurane was used to maintain the subject in the anesthesia state. Four 20-minute sessions of SSEPs were then consecutively recorded, with two sessions delivering stimulation to the left hindlimbs and the other two sessions to the right ones.

C. Time Domain Analysis of SSEP Peak Latencies

Time domain analysis of stimulation-triggered data captures by the TDT data acquisition system was performed with MNE-Python 1.6.1 [18]. Data snippets were imported as epochs and time-shifted -303 ms to align stimulation onsets with t=0, which included 3 ms compensation for observed hardware delay. Epochs were then cropped from -25 ms to 100 ms. DC shifts were de-trended, but baseline correction and re-referencing were not applied to preserve raw electrode activity. The time course of stimulation artifacts was examined by averaging over epochs and subsequently removed by linear interpolation between 0 ms and 7 ms. Epochs were then low-pass filtered using non-causal zero-phase FIR filters with a 100 Hz cutoff for ear electrodes and a higher 200 Hz cutoff for cortical electrodes to preserve high-frequency activity from

the cortical surface. Rejection criterion for peak amplitudes exceeding 100 µV on either cortical or ear electrodes within 7 ms to 100 ms was applied to drop epochs with intermittent artifacts, and epoch numbers were balanced between left and right stimulation conditions.

D. Wavelet Analysis of SSEP Time-Frequency Powers

SSEPs were evaluated for their properties in the frequency domain by applying wavelet transformation. The continuous wavelet transform (CWT) converts a one-dimensional signal in the time domain into a two-dimensional matrix of coefficients in the time-frequency domain:

$$C\big(a, b, S(t), \psi(t)\big) = \int_{-\infty}^{\infty} S(t) \frac{1}{a} \psi^* \left(\frac{t-b}{a} \right) dt \qquad (1)$$

where $S(t)$ is the original signal, a is the scale parameter, b is the translation parameter, $\psi(t)$ is the mother wavelet function, and $*$ is the complex conjugate operator. We select the Morse wavelet to perform the CWT and the resulting coefficients are used to make continuous time-frequency representations of SSEPs.

On the other hand, the discrete wavelet transform (DWT) is applied to quantify the relative powers of the commonly studied EEG sub-bands.

$$S(t) = \sum_{k=-\infty}^{\infty} a_N(k)\, \phi\left(2^{-N} t - k\right) + \sum_{j=1}^{N} \sum_{k=-\infty}^{\infty} C_j(k)\, \phi\left(2^{-j} t - k\right) \qquad (2)$$

In the above equation, $C_1(k), C_2(k), \ldots, C_N(k)$ are wavelet coefficients, and the sequence $a_N(k)$ represents the coarser resolution signal at level N [19], [20]. The DWT coefficients are used to compute the absolute and relative sub-band powers of SSEPs by the equations below:

$$E_j^{abs}(t) = \left| \sum_{k=-\infty}^{\infty} C_j(k,t) \right|^2 \qquad (3)$$

$$E_j^{rel}(t) = \frac{E_j^{abs}(t)}{\sum_{j=1}^{N} E_j^{abs}(t)} \qquad (4)$$

$C_j(t)$ represents the wavelet coefficients at the band level j and time t. We chose the *db5* wavelet family and a 6-level decomposition, from which we select the index j from 5 to 2 to extract the power of the theta (4 Hz-8 Hz), alpha (8 Hz-12 Hz), beta (12 Hz-30 Hz), and gamma (30 Hz-60 Hz), respectively.

E. Statistical Analysis

Welch's t-test was performed (MATLAB ver. 2023a) to compare EEG band powers between the ear and cortex recording. This method computes the t-statistic, a measure of the difference between the means of the groups relative to their within-group variability, and determines the degrees of freedom accordingly. Then, it calculates a p-value that represents the probability of observing the data under the null hypothesis of no difference between the group means. We used the significance level markers nf to indicate P>0.05, * to indicate P<0.05, and ** to indicate P<0.01.

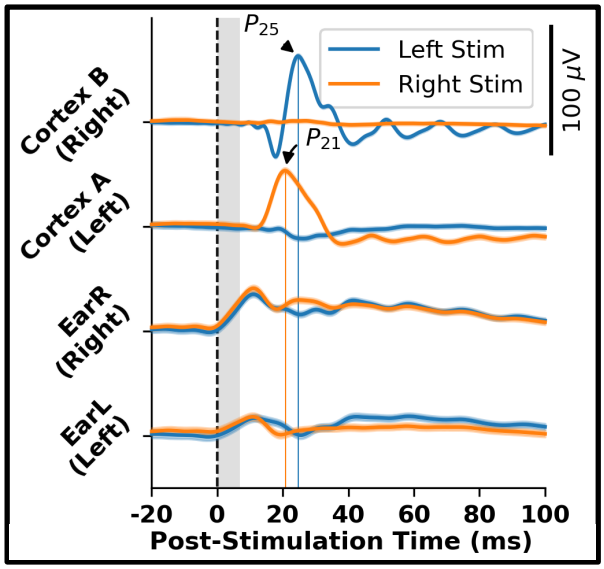

Fig. 2. Epoch-averaged SSEP activity comparing ear and cortical recordings for one rat subject under left (blue) and right (orange) hindlimb stimulation (Left Stim and Right Stim, respectively). Stimulation onset at t=0 (dashed black line). Low-pass filter cut-offs: 100 Hz for the ear and 200 Hz for the cortex. 294 epochs were averaged separately for each stimulation condition, with standard error as the shaded area under traces. Cortical electrodes show peak response in electrode locations contralateral to the stimulated hindlimb (Channel A contra. right hindlimb, Channel B contra. left hindlimb). Absolute peak latencies for cortical electrodes marked with thin vertical lines (A peak: orange, B peak: blue). The gray box shows 0 to 7 ms linear interpolation for stimulation artifact removal to adjust the vertical scale for visualization.

III. Results

A. SSEP Waveforms

Time traces of SSEPs for left and right hindlimb stimulation from one of three rat subjects are plotted in Fig. 2, as simultaneously recorded from cortical and ear electrodes. Cortical SSEPs for this subject show peak latencies of 25 ms (P25) and 21 ms (P21) for left and right hindlimb stimulation, respectively, as measured by contralaterally placed cortical electrodes B and A. Corresponding activity measured from the ears is shown below the cortex electrodes, with vertical markers aligning cortical peaks with corresponding ear activity. Fig. 3 shows the breakdown of individual epochs contributing to the SSEP for one stimulation condition (left hindlimb), and contralateral cortex and ear electrodes (Cortex B and EarR).

B. Time-Frequency Analysis

The wavelet coefficients computed by the CWT were used to generate the time-frequency heatmaps for the short-latency response (Fig. 4(a)). We observed that the cortical and ear SSEPs shared great similarities in terms of energy distributions, but the energy patterns of the ear SSEPs were shifted significantly earlier. On the other hand, the relative powers of the EEG sub-bands were computed by the DWT and illustrated in Fig. 4(b). Ear EEG recording results in significant power

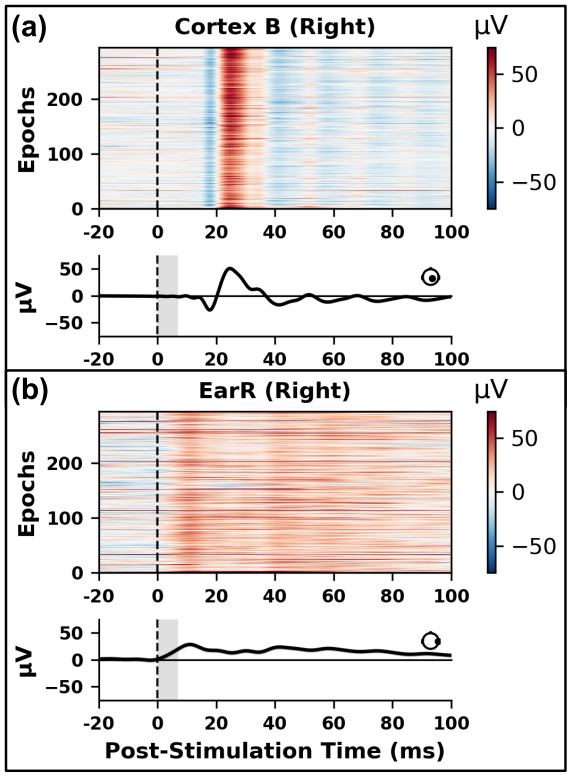

Fig. 3. Visualization of individual epochs from simultaneously recorded cortical and ear electrodes, both contralateral to left hindlimb stimulation in the same subject as Fig. 2. (a) Epochs and averaged SSEP for electrode B from the cortical surface, and (b) corresponding epochs and SSEP from an ear electrode placed in the right ear. The top panels of both sub-figures stack the same 294 epochs along the y-axis for both electrodes, with measured voltage amplitude over time mapped as color. The bottom panels show averaged SSEP, with linear interpolation of stimulation artifacts in gray boxes.

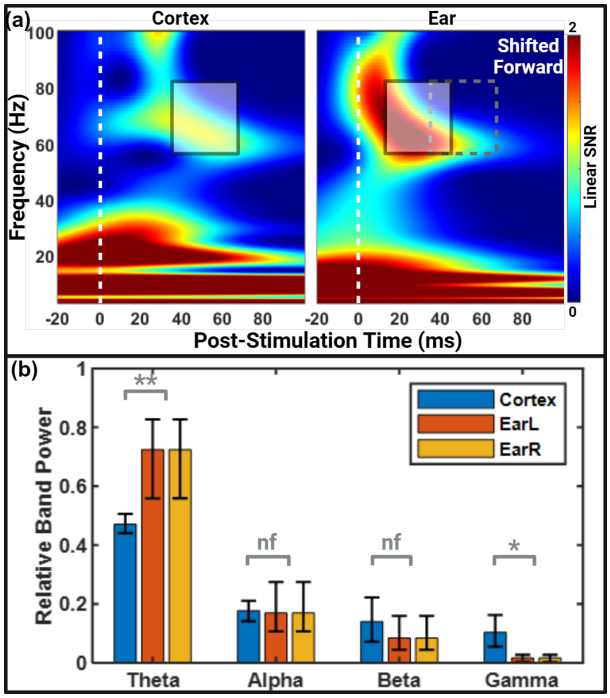

Fig. 4. (a) Grand average (N=3) of the time-frequency signal-to-noise ratio (SNR). The colors represent the linear SNR within a range of 0 (blue) to 2 (red). For the cortex heatmap, contralateral responses of both left stimulation sessions (channel B data) and right ones (channel A data) were used. For the ear heatmap, the mean of channels L and R was used regardless of the stimulation site. The shading areas capture a common energy pattern shared by both modalities. Nevertheless, the energy pattern was shifted earlier in the ear EEG recording. (b) Comparison of the relative EEG band powers between the recording modalities. Statistical significance markers: nf for $P>0.05$, * for $P<0.05$, and ** for $P<0.01$.

loss in the high-frequency domain. The SSEPs recorded from the ear EEG channels have a significantly larger relative theta band power (P=0.097) and a significantly smaller gamma band power (P=0.122). The two modalities recorded comparable alpha (P=0.897) and beta (P=0.539) powers.

IV. Discussion and Conclusion

As a step towards extending the prognostic utility of SSEPs beyond the clinic to ambulatory environments, this study explored recording SSEP activity from the ears of anesthetized rat subjects. SSEPs for left or right hindlimb stimulation were recorded from both ears, with simultaneous recording from the somatosensory cortex. Time and frequency domain analysis was performed to compare stimulation-epoched activity between the rat ears and cortex.

Time domain analysis showed weaker evoked activity in the ears, tracking the stronger cortical responses picked from the cortex contralateral to the stimulated hindlimb. Amplitude differences between cortical and ear electrodes are attributable to the weakening of the signal as it diffuses to the scalp [21]. Latency differences between cortex and ear electrodes are discussed below. SSEP waveform shape and latency differences between left and right stimulation, as measured by cortical electrodes, could be attributable to electrode location [22], or depth of anesthesia [23]. Differences between left and right ear signal strengths could be contact-related.

Wavelet analysis, on the one hand, found that the capacity of the ear SSEP recording decreases when the frequency of the desired activities increases, which is not surprising given that the skull acts as a low-pass filter [24]. On the other hand, the ear SSEP still kept a majority of the energy patterns below 100 Hz. Most interestingly, a prominent 60 Hz-80 Hz energy pattern was observed in both recording modalities, but the pattern in the ear appeared to occur at an earlier time, which is consistent with the shorter peak latency in the time domain.

The earlier occurrence of some SSEP components in the ear, compared to the cortex, may be attributable to the single-ended recording configuration used here (reference tied to ground). Several studies have demonstrated that the placement of the electrodes can reveal faster SSEP components in the far-field that are not apparent in the near-field SSEPs [25], [26]. It is also possible that the ear SSEP includes far-field contributions from subcortical structures anatomically closer to the ear [27], and earlier in the somatosensory pathway than the cortex. To test this hypothesis, future experiments with anesthesia modulation or injury induction would be necessary.

Current ear SSEP recording shares the limitations with the ones found in ear EEG, including low spatial resolution due to fewer electrodes, susceptibility to signal distortions

from motion artifacts and environmental interference, and challenges related to individual ear canal anatomy [28]. Some of these limitations can be resolved by improving the ear SSEP signal quality with biosignal amplification close to the ear electrodes, noise shielding, and contact impedance monitoring. Additionally, adaptive filtering can be applied to remove stimulation and ECG artifacts [29]. Besides, the results of this pilot study must be validated by future investigation with a larger sample size.

Ear SSEP could thus serve as a novel technique for monitoring neurological state in subsequent preclinical studies, with the bench-to-bedside translational impact of comprehensive in-ear brain monitoring for neurocritical care. The main advantage of ear devices is the fact that they are easy to use and can be set up quickly [12]. Follow-up research could examine whether ear SSEP could complement continuous EEG recordings in terms of assessing the integrity of sensory pathways and the severity of brain injuries. This will be a significant step towards the development of a comprehensive in-ear brain monitoring system in the next decade.

REFERENCES

[1] J. Madhok et. al., "Quantitative assessment of somatosensory-evoked potentials after cardiac arrest in rats," *Critical Care Medicine*, vol. 38, pp. 1709–1717, Aug. 2010.

[2] B. Lachance et. al., "Somatosensory evoked potentials and neuroprognostication after cardiac arrest," *Neurocritical Care*, vol. 32, pp. 847–857, June 2020.

[3] S. Benghanem et. al., "SSEP N20 and P25 amplitudes predict poor and good neurologic outcomes after cardiac arrest," *Annals of Intensive Care*, vol. 12, p. 25, Dec. 2022.

[4] E. Zandbergen et. al., "SSEPs and prognosis in postanoxic coma: only short or also long latency responses?," *Neurology*, vol. 67, pp. 583–586, Aug. 2006.

[5] Z. Ou at. al., "Time-frequency analysis of somatosensory evoked high-frequency (600 hz) oscillations as an early indicator of arousal recovery after hypoxic-ischemic brain injury," *Brain Sciences*, vol. 13, p. 2, Dec. 2022.

[6] D. Restuccia et. al., "Origin and distribution of P13 and P14 far-field potentials after median nerve stimulation. scalp, nasopharyngeal and neck recording in healthy subjects and in patients with cervical and cervico-medullary lesions," *Electroenceph. clin. Neurophysiol.*, vol. 96, pp. 371–384, Sept. 1995.

[7] M. R. Nuwer, "Spinal cord monitoring with somatosensory techniques:," *Journal of Clinical Neurophysiology*, vol. 15, pp. 183–193, May 1998.

[8] D. Ghatol and J. Widrich, "Intraoperative neurophysiological monitoring," in *StatPearls*, Treasure Island (FL): StatPearls Publishing, 2024.

[9] C. Tomberg, J. E. Desmedt, and I. Ozaki, "Right or left ear reference changes the voltage of frontal and parietal somatosensory evoked potentials," *Electroenceph. clin. Neurophysiol.*, vol. 80, pp. 504–512, Nov. 1991.

[10] Y. Xu et. al., "In-ear integrated sensor array for the continuous monitoring of brain activity and of lactate in sweat," *Nature Biomedical Engineering*, vol. 7, pp. 1307–1320, Sept. 2023.

[11] M. Masè, A. Micarelli, and G. Strapazzon, "Hearables: new perspectives and pitfalls of in-ear devices for physiological monitoring. a scoping review," *Frontiers in Physiology*, vol. 11, p. 568886, Oct. 2020.

[12] M. C. Yarici, M. Thornton, and D. P. Mandic, "Ear-EEG sensitivity modeling for neural sources and ocular artifacts," *Frontiers in Neuroscience*, vol. 16, p. 997377, Jan. 2023.

[13] P. Kidmose, D. Looney, and D. P. Mandic, "Auditory evoked responses from Ear-EEG recordings," in *IEEE EMBC 2012*, (San Diego, CA), pp. 586–589, IEEE, Aug. 2012.

[14] M. S. Lee et. al., "Scalable anatomically-tunable fully in-ear dry-electrode array for user-generic unobtrusive electrophysiology," in *IEEE EMBC 2023*, (Sydney, Australia), pp. 1–4, IEEE, July 2023.

[15] A. Paul et. al., "A versatile in-ear biosensing system and body-area network for unobtrusive continuous health monitoring," *IEEE Transactions on Biomedical Circuits and Systems*, vol. 17, pp. 483–494, June 2023.

[16] A. Curt and V. Dietz, "Ambulatory capacity in spinal cord injury: significance of somatosensory evoked potentials and ASIA protocol in predicting outcome," *Archives of Physical Medicine and Rehabilitation*, vol. 78, pp. 39–43, Jan. 1997.

[17] M. S. Lee, A. Paul, Y. Xu, W. D. Hairston, and G. Cauwenberghs, "Characterization of Ag/AgCl Dry Electrodes for Wearable Electrophysiological Sensing," *Frontiers in Electronics*, vol. 2, Jan. 2022. Publisher: Frontiers.

[18] A. Gramfort et. al., "MEG and EEG data analysis with MNE-Python," *Frontiers in Neuroscience*, vol. 7, 2013.

[19] H. A. Al-Nashash et. al., "Wavelet entropy for subband segmentation of EEG during injury and recovery," *Annals of Biomedical Engineering*, vol. 31, pp. 653–658, June 2003.

[20] O. A. Rosso et. al., "Wavelet entropy: a new tool for analysis of short duration brain electrical signals," *Journal of Neuroscience Methods*, vol. 105, pp. 65–75, Jan. 2001.

[21] Broughton, "The relationship of brain activity to scalp recordings of event-related potentials," in *Average Evoked Potentials; Methods, Results, and Evaluations* (E. Donchin and D. B. Lindsley, eds.), ch. 2, pp. 79–84, Washington, D.C.: National Aeronautics and Space Administration, 1969.

[22] K. Sakatani, H. Iizuka, and W. Young, "Somatosensory evoked potentials in rat cerebral cortex before and after middle cerebral artery occlusion," *Stroke*, vol. 21, pp. 124–132, Jan. 1990.

[23] J. Kortelainen et. al., "Effect of isoflurane on somatosensory evoked potentials in a rat model," in *IEEE EMBC 2014*, (Chicago, IL), pp. 4286–4289, IEEE, Aug. 2014.

[24] R. Srinivasan, D. M. Tucker, and M. Murias, "Estimating the spatial Nyquist of the human EEG," *Behavior Research Methods, Instruments, & Computers*, vol. 30, pp. 8–19, Mar. 1998.

[25] E. Urasaki, S.-i. Wada, C. Kadoya, A. Yokota, S. Matsuoka, and F. Shima, "Origin of scalp far-field N18 of SSEPs in response to median nerve stimulation," *Electroencephalography and Clinical Neurophysiology/Evoked Potentials Section*, vol. 77, pp. 39–51, Jan. 1990.

[26] M. Kritchevsky and W. C. Wiederholt, "Short-Latency Somatosensory Evoked Potentials," *Archives of Neurology*, vol. 35, pp. 706–711, Nov. 1978.

[27] L. W. Swanson, "*Brain Maps 4.0—Structure of the rat brain* : An open access atlas with global nervous system nomenclature ontology and flatmaps," *Journal of Comparative Neurology*, vol. 526, pp. 935–943, Apr. 2018.

[28] T. Röddiger, C. Clarke, P. Breitling, T. Schneegans, H. Zhao, H. Gellersen, and M. Beigl, "Sensing with Earables: A Systematic Literature Review and Taxonomy of Phenomena," *Proceedings of the ACM on Interactive, Mobile, Wearable and Ubiquitous Technologies*, vol. 6, pp. 1–57, Sept. 2022.

[29] P. Agarwal, Y. Guo, and N. V. Thakor, "Advancing Ear ECG Analysis during CPR Using Adaptive Filtering," in *2023 IEEE Biomedical Circuits and Systems Conference (BioCAS)*, pp. 1–5, Oct. 2023. ISSN: 2766-4465.